JOURNAL OF PLANKTON RESEARCH | VOLUME 28 | NUMBER 5 | PAGES 437–448 | 2006

What determines the slope of a plankton biomass spectrum?

MENG ZHOU

DEPARTMENT OF ENVIRONMENTAL, EARTH AND OCEAN SCIENCES, UNIVERSITY OF MASSACHUSETTS BOSTON, 100 MORRISSEY BOULEVARD, BOSTON, MA 02125, USA

CORRESPONDING AUTHOR: meng.zhou@umb.edu

Received August 3, 2005; accepted in principle November 16, 2005; accepted for publication January 3, 2006; published online January 10, 2006

Communicating editor: I.R. Jenkinson

A number of studies have been performed to understand the characteristics of biomass (size) spectra in aquatic plankton communities around the world. Although the area below a biomass spectrum curve represents the abundance or biomass of a plankton community, it has been hypothesized that the slope and shape of a biomass spectrum are determined by rates of growth, respiration, mortality and trophic dynamics. Observations of biomass spectra indicate that the slope of a biomass spectrum is around –1 on the logarithmic coordinates. Empirical hypotheses of growth-survival and the theoretical framework on biomass conservation based on the rates of individual body growth and abundance change have been developed for interpreting the slope and domes of a biomass spectrum. Here, a mathematical method is developed for estimating specific rates of body growth and abundance change from observations of biomass spectra, and a mathematical model is constructed for the relationship between a biomass spectrum slope, community assimilation efficiency and trophic levels.

INTRODUCTION

The productivity of a plankton community is apparently determined by rates of body growth and abundance change, which are in turn determined by food availability and trophic relations, that is, the community structure. For a community consisting of a number of species and trophic links, it is a daunting task to take the traditional approach for predicting productivity by determining individual body and stage development, birth and mortality rates of each species and stage, and relationships between prey and predators. In examples of estimating growth rates alone, the measured growth rates of copepods have a 95% confidence interval of five times the mean value from compiling all existing 181 measurements over 33 species in different oceans conducted during last several decades (Hirst and Lampitt, 1998). Measurements of other species are even rare. Although these results have successfully elucidated basic processes of individuals, extrapolating these results to predict community productivity is definitely questionable because of significant uncertainties in rate estimates. If we imagine that each of these experiments contained 10^2 individuals, all these experiments used 10^4 individuals in last several decades. The total area of the global ocean is $\sim 3.6 \times 10^{14}$ m^2. If we assume that the mean abundance of mesozooplankton in the upper 100 m is on the order of 10^3 individuals m^{-3}, the number of total mesozooplankton is on the order of 10^{19} individuals in the global ocean. It is obviously doubtful that the results of those 10^4 experimented copepods could represent the mean and variance of mesozooplankton in the oceans even if these results could be obtained all at once. It is even more problematic to find trophic links between species and stages. A productivity model based on species faces unconquerable challenges for being practically applicable to most natural ecosystems due to variations of individual behavior and community structure complexity (Jorgensen, 1990, 1994).

The most unpredictable uncertainty is the prey–predator relationship because it varies with variations in physical, biochemical and biological environmental parameters. Many grazers may feed on whatever is available for them instead of seeking their preferred food which may never be available during their life time. For example, Antarctic krill, *Euphausia superba*, change their primary diet from

This paper was presented in a session on "Size Structure of Plankton Communities", at the ASLO Summer International Meeting, held in Santiago de Compostela, Spain, between 19 and 24 June, and coordinated by Xabier Irigoien, Roger Harris and Angel Lopez-Urrutia.

doi:10.1093/plankt/fbi119, available online at www.plankt.oxfordjournals.org

© The Author 2006. Published by Oxford University Press. All rights reserved. For Permissions, please email: journals.permissions@oxfordjournals.org

Downloaded from https://academic.oup.com/plankt/article/28/5/437/1457472 by guest on 21 August 2022

phytoplankton in spring, summer and autumn to other zooplankton in winter (Hopkins *et al.*, 1993; Huntley *et al.*, 1994a; Atkinson and Snyder, 1997; Atkinson *et al.*, 2002; Zhou *et al.*, 2004). Especially, for microzooplankton and mesozooplankton which have limited swimming capability, food supplies rely primarily on local production and biota transported by advection and mixing. A plankton community has spatial and temporal scales from the neighboring distance between plankton of 10^{-3} m to a regional sea of 10^5 m and from escaping of 10^0 s for avoiding a predator to seasonal change of 10^2 days. Many of those small spatial and temporal scale processes are stochastic, unpredictable and immeasurable. Thus, statistically mean variables and process rates are needed to represent stochastic processes, and mathematical theories need to be developed based on these statistically meaningful variables and rates.

One such statistical approach is to classify plankton on the basis of size (Sheldon and Parsons, 1967; Sheldon *et al.*, 1972, 1977). In early empirical work, graphs of abundance versus size show a trend of a peak abundance at the low end of a size spectrum and a quick decrease to a relatively minuscule abundance at large size (Sheldon *et al.*, 1972; Rodríguez and Mullin, 1986; Sprules and Munawar, 1986). The classification of plankton on the basis of size alone greatly simplifies the community structure and allows individual growth and abundance change be estimated from allometrically scaled rates (Fenchel, 1974; Huntley and Boyd, 1984; Hirst and Lampitt, 1998). To understand the trophic relationship, size-dependent processes have been examined, showing the different slopes and domes for different trophic groups on a size spectrum (Dickie *et al.*, 1987; Sprules and Munawar, 1986; Sprules *et al.*, 1991). These studies have indicated that the averaged biomass spectrum from a particular region is linear or near linear.

Two of the most important advantages in using the size-based classification are (i) to allow the use of automated counting instruments for measuring plankton *in situ* (Herman, 1988; Heath, 1995; Huntley *et al.*, 1995; Herman *et al.*, 2004) and (ii) to allow the use of advanced mathematics for expressing population processes (Edvardsen *et al.*, 2002; Platt and Denman, 1978; Silvert and Platt, 1978; Heath, 1995; Zhou and Huntley, 1997). With the increased capacity in resolving spatial and temporal distributions of plankton size structure in a natural ecosystem, mathematical theories have been developed, intended to interpret the change of a size spectrum in terms of growth, respiration, survival and mortality.

One critical step in developing mathematical theories is to define the so-called normalized biomass spectrum (Platt and Denman, 1978; Silvert and Platt, 1978), that is, in a unit water volume (m^3) (referred to hereafter as biomass spectrum)

$$\text{Biomass spectrum}(b) = \frac{\text{Biomass}(\mu\text{gC})\text{in the size interval}(\Delta w)}{\text{The size}(\mu\text{gC})\text{interval}(\Delta w)}(\text{m}^{-3}) \quad (1)$$

where the biomass within a given size interval (Δw) is expressed in terms of carbon, and the body biomass (w) of a plankter is also in carbon, the common currency between size groups and different functional groups. Because the units of the numerator and denominator in the definition [equation (1)] cancel each other out, the unit of a biomass spectrum (b) is in m^{-3}. Using this definition, the biomass spectrum is unique for a given size-structured plankton community and independent of the subjective sorting size intervals (Kerr and Dickie, 2001). In a case that the relation between body size and carbon is unknown, a biovolume spectrum can be used simply, replacing the biomass in equation (1) by the biovolume of organisms (Edvardsen *et al.*, 2002; Quinones *et al.*, 2003; Zhou *et al.*, 2004).

The studies of biomass spectra in inland lakes and oceans have demonstrated that the relationship between the biomass spectrum of a plankton community and body size is nearly linear. *In situ* observations of biomass spectra have shown that the slopes vary from –0.6 in southeastern Lake Superior (Zhou *et al.*, 2001), 0.90 to –1.16 in inland lakes (Sprules and Munawar, 1986), −1.23 for microplankton and –1.13 for macrozooplankton in the north Pacific Central Gyre (Rodríguez and Mullin, 1986) to –1.5 in the California Current (Huntley *et al.*, 1995; Zhou and Huntley, 1997). Significant efforts have been made to interpret the meaning of biomass spectrum slopes in terms of growth, mortality, respiration and survival by both empirical relations (Dickie *et al.*, 1987; Beyer, 1989; Heath, 1995) and theoretical relations (Platt and Denman, 1978; Silvert and Platt, 1978; Zhou and Huntley, 1997).

The first empirical model of the slope was given by Platt and Denman (Platt and Denman, 1978). In their model, the slope (β) of a biomass spectrum consists of

$$\beta = -(1 - x + \alpha A + q) \quad (2)$$

where x is the turnover time of body weight, αA is the time scale of system energy loss and q is an exponent for feeding efficiency. The analysis was based on allometrically scaled rates. The basic slope of a biomass spectrum is hypothesized to be –1, and other constants are exponents of allometrically scaled rates, representing the corrections due to different processes. The range of slopes was predicted between –0.82 and –1.23. The theoretical development indicates that the slope of a biomass spectrum is proportional to the ratio of specific abundance

Downloaded from https://academic.oup.com/plankt/article/28/5/437/1457472 by guest on 21 August 2022

change to individual body growth rates (Zhou and Huntley, 1997). In a time-dependent case, cohorts can propagate along the size spectrum (Silvert and Platt, 1978; Zhou and Huntley, 1997).

The problem in applying any biomass spectrum theory is to have the *in situ* rates of abundance change within size classes, which in many cases are determined by prey–predator relations. Studies on trophic interactions have been made on the basis of analysis of dome-like features in a biomass spectrum (Sprules and Munawar, 1986; Dickie *et al.*, 1987; Sprules and Stockwell, 1995). However, assuming a constant size relationship between prey and predators is quite ambiguous and error-prone (Longhurst, 1989, 1991; Thiebaux and Dickie, 1993). Since the realization that the time-dependent variation of a biomass spectrum represents the dynamics and imbalance between population processes within a plankton community, such as growth, birth and mortality, inverse mathematical methods have been developed to understand the growth and mortality processes and to solve individual body growth and mortality rates based on a sequence of observations (Heath, 1995; Edvardsen *et al.*, 2002; Zhou *et al.*, 2004).

The increase in measurements of biomass spectra within lakes and oceans has allowed us to examine the common features and variations in observed biomass spectra, and the development of mathematical theories and inverse methods has allowed us to access *in situ* growth and mortality rates and to seek causes for the variation of biomass spectrum slopes. The purpose of this work was to develop a biologically meaningful mathematical method for estimating *in situ* rates of body growth and abundance change as well as a community structure index for the relationship between the community-assimilation efficiency, trophic levels and the slope(s) of the biomass spectrum within a plankton community.

METHODS: BASIC EQUATIONS

The body growth of a plankter and the abundance change indicate a biomass flow from small-to-large sizes and birth–death, respectively, which determine the productivity of an aquatic plankton community. Here we adopt the continuum model developed by Silvert and Platt (Silvert and Platt, 1978) and Zhou and Huntley (Zhou and Huntley, 1997), which explicitly use statistically mean rates of individual growth and abundance change. The detailed mathematical development can be found in Zhou and Huntley (Zhou and Huntley, 1997). Here, we briefly outline the basic equations and deductions. In the continuum model, the biomass flow can be generally expressed by a time-dependent partial differential equation, that is

$$\frac{\partial b}{\partial t} + \frac{\partial (wgb)}{\partial w} = (\mu + g)b, \tag{3}$$

where g is the mean specific individual growth rate defined as $(1/w)(\mathrm{d}w/\mathrm{d}t)$, μ is the mean specific rate of net abundance change defined as $(1/N)(\mathrm{d}N/\mathrm{d}t)$, N is the number of plankton at size (w) and b is the biomass or biovolume spectrum defined by equation (1). Equation (3) is an exact mathematical expression of the biomass balance: the first term on the left is the rate of change in biomass at a given size, and the second term on the left is the propagation of biomass crossing the size spectrum at the rate of body growth, the first term on the right represents the birth and mortality, and the second term on the right represents the individual growth. Because plankton abundance and biomass exponentially decrease from small-to-large sizes, most biomass spectra are expressed in logarithmic coordinates. Normalizing equation (3) by the biomass spectrum (b), and rearranging after taking partial derivatives of the second term on the left side, we have

$$\frac{\partial \ln b}{\partial t} + g\frac{\partial \ln b}{\partial \ln w} = \mu - \frac{\partial g}{\partial \ln w}, \tag{4}$$

where we use the natural logarithms for the mathematical convenience, although logarithms to the base 10 are commonly used in plankton studies. The time scales of the terms in equation (4) can be estimated from specific processes. The first term on the left is typically determined by the time scale of interest such as the seasonal and annual scales; the second term on the left is determined by the time scale of growth $(1/g)$ that varies from days to 10s of days primarily determined by temperature and size (Huntley and Boyd, 1984; Huntley and Lopez, 1992; Hirst and Lampitt, 1998); the first term on the right is determined by the time scale of abundance change $(1/\mu)$ that also varies from days to 10s of days (Fenchel, 1974; Miller *et al.*, 1984; Huntley *et al.*, 1994b; Ohman and Aksnes, 1996; Ohman and Wood, 1996; Edvardsen *et al.*, 2002), and the second term on the right is the spreading of biomass along the size spectrum due to size-dependent growth (Hirst and Sheader, 1997; Hirst and Lampitt, 1998). Size-dependent growth can be expressed as

$$g = e^{aT_{em}^{-b}} w^{-c} \tag{5}$$

where a, b and c are empirical constants, and T_{em} is the temperature. Differentiating equation (5) related to $\ln(w)$, we have

$$\frac{\partial g}{\partial \ln w} = -c \cdot g, \tag{6}$$

Downloaded from https://academic.oup.com/plankt/article/28/5/437/1457472 by guest on 21 August 2022

where the constant c is estimated between 0.0795 for juvenile copepods to 0.3569 for adult copepods (Hirst and Sheader, 1997; Hirst and Lampitt, 1998). Thus, the time scale associated with size-dependent variations in growth is 3–10 times longer than the mean growth and mortality. In the case that the growth is only temperature dependent (Huntley *et al.*, 1994b), the derivative [equation (6)] is equal to zero. In some analyses, equation (4) is simplified by ignoring this size-dependent growth (Zhou and Huntley, 1997; Edvardsen *et al.*, 2002). Such a simplification is not necessary. In the following analyses, this term [equation (6)] is included.

RESULTS

Steady-state solutions

When a size-structured population reaches a steady state, equation (4) can be simplified as

$$\frac{\partial \ln b}{\partial \ln w} = \frac{\mu}{g} - \frac{\partial \ln g}{\partial \ln w}. \tag{7}$$

Substituting the approximation of equation (6) into equation (7), we have

$$\frac{\partial \ln b}{\partial \ln w} = \frac{\mu}{g} + c. \tag{8}$$

Thus, the slope of a biomass spectrum will be reduced by ~0.1 for juvenile copepods and 0.4 for adult copepods due to size-dependent growth on the basis of the variation of constant c in equation (5) (Hirst and Sheader, 1997; Hirst and Lampitt, 1998). This conclusion can be only used for demonstrating the influence of size-dependent growth on the slope of a biomass spectrum associated with copepods.

Equation (7) can be applied to a general plankton community. If we are able to measure *in situ* individual growth rates as a function of size and the slope of a plankton community, the corresponding *in situ* rate of abundance change can be inferred by rearranging equation (7), that is,

$$\mu = g\left(\frac{\partial \ln b}{\partial \ln w} + \frac{\partial \ln g}{\partial \ln w}\right) = g\frac{\partial \ln(gb)}{\partial \ln w}. \tag{9}$$

The general solution of equation (7) can be written as

$$\frac{b}{b_1} = \left(\frac{g_1}{g}\right) e^{\int_{w_1}^{w} \frac{\mu}{g} \ln w}, \tag{10}$$

where w_1, b_1 and g_1 are the reference point on a biomass spectrum, which are simply determined by the smallest plankton observed in samples. In most of observations, the linearity of a biomass spectrum does not imply a linear relation between μ and g. For a linear biomass spectrum, equation (7) can be integrated directly that leads to the general solution,

$$\frac{b}{b_1} = \left(\frac{w}{w_1}\right)^{\frac{\mu}{g} + \frac{\partial \ln g}{\partial \ln w}}. \tag{11}$$

This solution is a better one than the solution assuming a constant ratio of μ to g if g and μ are size dependent.

Time-dependent solutions

Equation (4) can be solved when g and μ are time independent such as within a season. The solution of equation (4) can be split into two parts, a time-independent state solution (b^*) of equation (9) and a time-dependent solution (b'), that is

$$\ln b = \ln b^* + \ln b', \tag{12}$$

where b' is nondimensional and satisfies with

$$\frac{\partial \ln b'}{\partial t} + g\frac{\partial \ln b'}{\partial \ln w} = 0, \tag{13}$$

which is a simple first-order wave equation. For investigating the basic characteristic, we assume that g is size-independent. Then the general solution of this equation is

$$\ln b' = f(\ln w - gt), \tag{14}$$

where f is an arbitrary continuous function. Given the initial condition $b(w, t = 0) = b_0(w)$, we have the solution of equation (4),

$$\ln b = \ln b_0(\ln w - gt) + \mu t, \tag{15}$$

The first term on the right represents the propagation of biomass in an enclosed community along the axis of $(\ln w)$, shifting an initial biomass spectrum from the left to the right without any change in the shape. The second term represents the exponential decay of biomass due to the reduction of abundance, which shifts the biomass spectrum downward. When g is a size-dependent function, equation (13) can be solved numerically. It should be noted that in an open community with import and export of plankton driven by physical processes such as advection, the contribution by such physical processes to changes in biomass spectra must be removed first before these equations can be applied (Zhou, 1998; Edvardsen *et al.*, 2002).

Downloaded from https://academic.oup.com/plankt/article/28/5/437/1457472 by guest on 21 August 2022

Trophic levels versus ecosystem productivity efficiency

The slope of a biomass spectrum is determined by equation (7) when a plankton community reaches its stable state. Then, what determines the relations between individual growth and abundance change? The body growth of individuals requires constant supplies of biomass (energy), which can be provided from external and internal sources. An internal source is defined as the certain amount of plankton biomass fed by next trophic level organisms in a plankton community, that is, the biomass has been recycled internally. For a system defined by the size range larger than w_1, the biomass fluxes include (i) the biomass import from the left side of w_1, (ii) the biomass removal from net mortality including birth, death and predation, (iii) the recycles of the biomass between different trophic levels and (iv) the growth of all individuals (Fig. 1). The first flux is the biomass supplied from the outside of a system, and the second flux is the internal biomass recyclable. These four fluxes can be written as

$$(wgb)|_{w_1},\quad \int_{w_1}^{\infty}\mu b\,\mathrm{d}w,\quad -(n-1)\int_{w_1}^{\infty}\mu b\,\mathrm{d}w \quad \text{and} \quad \int_{w_1}^{\infty} gb\,\mathrm{d}w, \tag{16}$$

respectively, where n is equivalent to the number of trophic levels within which the internal biomass is recycled $n-1$ times. Thus, the assimilation efficiency (η_n) of the community is equal to

$$\eta_n = \frac{\int_{w_1}^{\infty} gb\,\mathrm{d}w}{(wgb)_{w_1} - (n-1)\int_{w_1}^{\infty}\mu b\,\mathrm{d}w}. \tag{17}$$

Substituting equation (11) into equation (17) and integrating, we have

$$\eta_n = \frac{1}{1 + n(\partial \ln b/\partial \ln w)}, \tag{18}$$

or

$$n = \frac{1+\eta_n}{\eta_n(\partial \ln b/\partial \ln w)}. \tag{19}$$

From equation (18), we can estimate the energy utilization efficiency by knowing the number of trophic levels and slope of a biomass spectrum, or we can reversely estimate the number trophic levels on the basis of equation (19) from the system-productivity efficiency and slope of a biomass spectrum. The theoretical curves of the biomass recycles, slope of a biomass spectrum and assimilation efficiency are shown in Fig. 2.

APPLICATIONS AND DISCUSSION

A steady state versus temporal average

The nature of equation (4) is a forced wave equation. Any perturbation such as changes in g, μ or b will lead to a wave propagating through the size spectrum at a traveling rate of g, a dumping rate of μ and a spreading rate of $(\partial g/\partial \ln w)$. These rates should be sensitive to seasonal temperature changes, life histories and primary

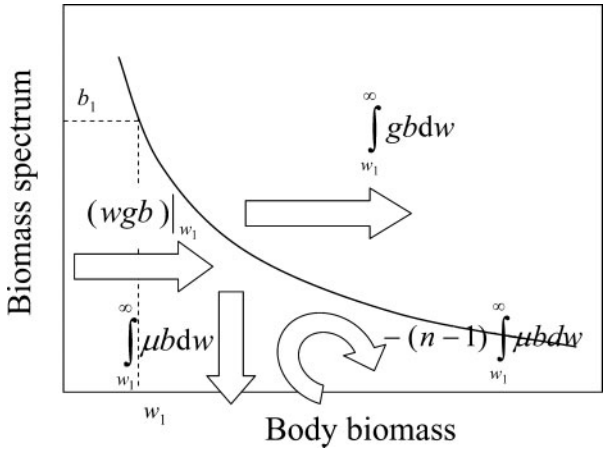

Fig. 1. A sketch of biomass fluxes through a biomass spectrum.

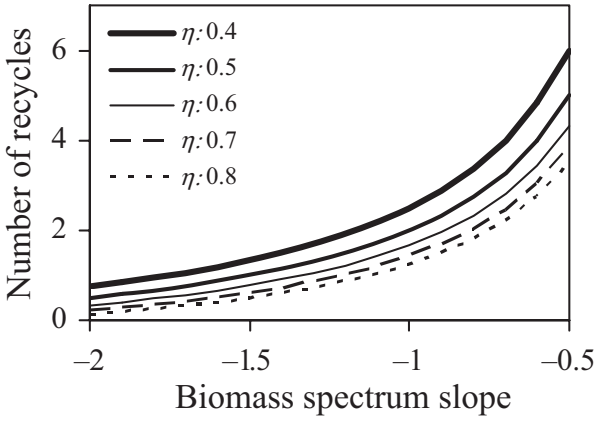

Fig. 2. Theoretically predicted numbers of recycles versus slopes of biomass spectra at different community assimilation efficiencies.

Downloaded from https://academic.oup.com/plankt/article/28/5/437/1457472 by guest on 21 August 2022

production. We can image that in a community a generation of copepods propagates from a small size of their egg to a large size of adults and then reproduces eggs into the small size. Such a process is time dependent, and the size spectrum will never reach a steady state. We can argue that when more species and generations appear in a community, the biomass spectrum may be close to a steady state. But it is hard to argue with the seasonality that the growth, reproduction and behavior of many plankton species are temperature dependent. Then what is the value of a steady-state solution of equation (8)?

The time scales associated with these rates, μ and g, are $\sim 10^1$ days which are one order of magnitude less than the seasonal scale of 10^2 days. Taking the time average of equation (4) over a seasonal scale, we have

$$\frac{\partial \ln b_t}{\partial \ln w} = \frac{\mu_t}{g_t} - \frac{\partial \ln g_t}{\partial \ln w}, \tag{20}$$

where the subscript 't' indicates a temporal average. Thus, even if there is no absolute steady-state solution, equation (20) indicates that the seasonal means are satisfied with the steady-state solution of equation (8). This temporal average can sometimes be replaced by a spatial average if we assume that short temporal variations are similar to spatial variations (Zhou and Huntley, 1997). Note that during the development of equation (20), there is no assumption that the biomass spectrum is linear. Having equation (20) is the key step to solve growth and mortality rates.

Estimating growth and mortality rates

One of the key issues in predicting ecosystem productivity is to have a practical means to estimate rates of individual body growth and abundance change. Although the individual growth can be estimated from *in situ* and laboratory experiments, the applicability of estimated rates to *in situ* cases is difficult to determine. Estimation of *in situ* rates of abundance change cannot be done by any experiments and is hardly ever achieved. However, in a field study, Edvardsen *et al.* (Edvardsen *et al.*, 2002) demonstrated that by taking a time sequence of biomass (biovolume) spectrum measurements, *in situ* rates of individual growth and mortality can be estimated. The mathematical methods used for those estimates were well developed in that study, while the biological processes were buried in those mathematical symbols. The difficulty in that approach is the requirement for at least three statistically independent biomass spectrum measurements in a time sequence which requires an extensive field observation period. Here, a new approach is introduced, which is based on the biologically meaningful computations developed in the *Methods* and *Results* sections and requires only two sequential biomass spectrum measurements so that we can cut the observation period to half.

Subtracting equation (20) from equation (4) and assuming g and μ are time independent similar to the seasonal means, we have

$$\frac{\partial \ln b}{\partial t} + g_t\left(\frac{\partial \ln b}{\partial \ln w} - \frac{\partial \ln b_t}{\partial \ln w}\right) = 0 \tag{21}$$

Recalling equation (12) and assuming

$$\ln b' = \ln b - \ln b_t, \tag{22}$$

where b' is the nondimension anomaly to the seasonal mean, we have

$$\frac{\partial \ln b'}{\partial t} + g_t \frac{\partial \ln b'}{\partial \ln w} = 0 \tag{23}$$

Because this anomaly equation only represents the propagation of anomalies at a rate of g_t, the individual growth rate (g_t) can be solved without dealing with the rate of abundance change (μ_t) by using a time sequence of biomass spectrum measurements. After solving g_t, equation (9) can be used to solve μ_t.

To demonstrate these procedures, we use biovolume spectra of the zooplankton community in Sørfjorden, Norway which were used in Edvardsen *et al.* (Edvardsen *et al.*, 2002). Three spectra were taken on 13 May, 3 June and 16 June 1998 from fjord-wide mappings by using an Optical Plankton Counter (OPC; Focal Technologies, Dartmouth, Nova Scotia, Canada) mounted on a towed Scanfish (Chelsea Instruments, Chelsea, UK). It is difficult to identify any wave propagation from these three biovolume spectra (Fig. 3).

We first take the mean of these three biovolume spectra and then divide these three biovolume spectra by the mean (Fig. 3). Now, the anomalies provide a much better view of a propagation of a cohort along the size spectrum: a cohort in the size range between $10^{-1.4}$ mm^3 and $10^{1.0}$ mm^3 propagated to the size range between $10^{0.8}$ mm^3 and $10^{2.4}$ mm^3 in a period of 21 days from 13 May to 3 June 1998 and to the size range between $10^{1.1}$ mm^3 and $10^{2.8}$ mm^3 in a period of 14 days from 3 June to 16 June 1998.

From such an analysis, the propagation rates can be directly estimated from the size changes ($\Delta \ln b'$) versus time intervals (Δt), that is,

Downloaded from https://academic.oup.com/plankt/article/28/5/437/1457472 by guest on 21 August 2022

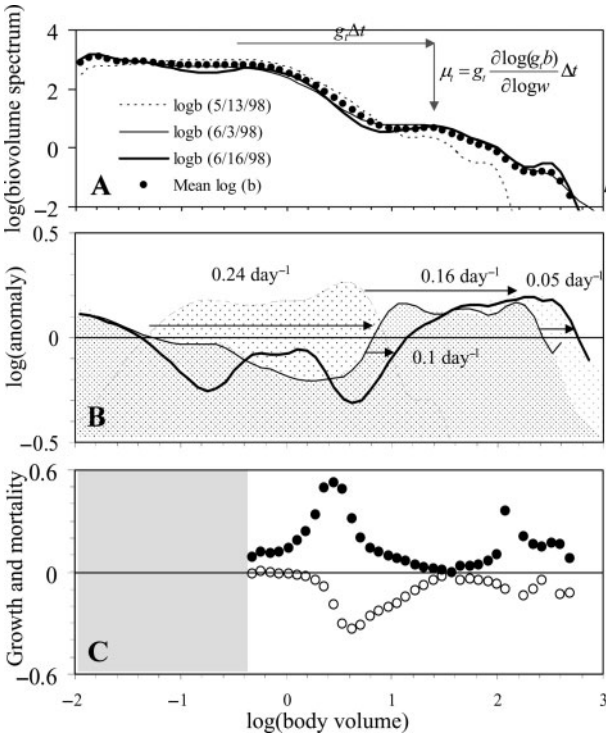

Fig. 3. Biovolume spectra in m^{-3} (**A**), nondimensional biovolume spectrum anomaly (**B**) and estimates of body growth and mortality rates in day^{-1} (**C**) as a function of body size in mm^3 within Sørfjorden, Norway during May and June, 1998. Arrows in **A** and **B** elucidate the cohort propagation from small-to-large sizes and decrease in abundance due to mortality; shaded areas in **B** represent the cohorts; numbers in **B** are the estimates of body growth rates indicated by those arrows; and no rate estimates can be made in the shaded area in **C** due to the CFL condition. All axes are 10-based logarithmic.

$$g = \frac{\Delta \ln b'}{\Delta t}. \tag{24}$$

The cohort propagated at the growth rate from 0.16 to 0.24 day^{-1} between 13 May and 3 June 1998, and from 0.05 to 0.1 day^{-1} between 3 June and 16 June 1998 (Fig. 3). These rates are consistent with those estimated in Edvardsen *et al.* (Edvardsen *et al.*, 2002).

More sophisticated mathematical methods can be used. For example, finite differences can be used to replace the differentials in equation (23), that is,

$$g_t = -\frac{\Delta \ln b'/\Delta t}{\Delta \ln b'/\Delta \ln w}. \tag{25}$$

To solve g_t, we now need only two sequential measurements of biovolume spectra for the time difference in equation (25). Using biovolume spectrum measurements on 3 June and 16 June 1998, the growth rate can be computed on the basis of equation (25) (Fig. 3). In the next step, the rate of abundance change, that is the mortality rate here, can be computed by

$$\mu_t = g_t\left(\frac{\partial \ln b_t}{\partial \ln w} + \frac{\partial \ln g_t}{\partial \ln w}\right). \tag{26}$$

Because equation (25) is based on a first-order wave equation [equation (23)], the attention must be paid to the Courent-Friedrich-Lewy (CFL) stability condition during the computation for ensuring the convergence of its solution (Marchuk, 1975; Edvardsen *et al.*, 2002). That is, when computing the slope of a biovolume spectrum in equation (25), $\Delta \ln w$ must be chosen by the condition,

$$\Delta \ln w > g_t \Delta t. \tag{27}$$

Because we do not know g_t initially, several trials are needed by judging if the estimated value of $g_t\Delta t$ is close to $\Delta \ln w$ used.

In a brief summary, the computational steps include (i) obtaining the biovolume (biomass) spectrum anomalies by removing the seasonal mean to obtain the propagation of cohorts [equation (22)]; (ii) estimating the individual growth rate (g_t) based on equation (25) while paying attention to Condition 27, which simply estimates how far these cohorts had propagated on the size spectrum between two surveys (Fig. 3); and (iii) estimating the rate of abundance change (μ_t) based on equation (26), which simply estimates how much biovolume (biomass) has been lost during the propagation.

The results of these rate estimates are very similar to those published in Edvardsen *et al.* (Edvardsen *et al.*, 2002), which show that during the survey period *Calanus finmarchicus* at CV and euphausiid calyptopes and furcilia dominated the size range between 0.58 and 4 mm^3 where the growth rates reached a peak of 0.59 day^{-1}. Such a fast grow is a rarely documented phenomenon (Brinton and Townsend, 1991). The predators in the fjord were dominated by chaetognaths (*Sagitta elegans*), which were up to 40 individuals m^{-3} (Zhou *et al.*, 2005). Their predation on *C. finmarchicus* and euphausiid calyptopes and furcilia led to enhanced mortality within this size range.

The advantage of this method is that only two biomass spectrum measurements are needed with the payback that we must know the seasonally mean biomass spectrum. We should take this as a positive side of this method because it signifies the need for long-term observations of biomass spectra in different regions so that we can have population rate estimates and understand the seasonal evolution of community structures.

Downloaded from https://academic.oup.com/plankt/article/28/5/437/1457472 by guest on 21 August 2022

Slope of a biomass spectrum versus trophic levels

The characteristics of a biomass spectrum can mathematically be described by the intercept and slope of the curve. The intercept represents the abundance of plankton. Growth, mortality and trophic levels of a plankton community can be obtained from analysis of the slope, that is, equations 18 and 19. These two Equations simply link the community assimilation efficiency (η_n) and trophic levels to the slope of a biomass spectrum (Figs 1 and 2).

The community assimilation efficiency should be similar to the mean individual assimilation efficiency. Taking the notations by Kerr and Dickie (Kerr and Dickie, 2001), the net growth efficiency (K) of an organism is equal to

$$K = \frac{PC - T}{PC}, \tag{28}$$

where T is the total metabolic dissipation, and PC is the total carbon intake. The difference ($PC-T$) is equal to the growth ($g \cdot w$). For a community, the mean of equation (28) for all plankton should be equivalent to the community-assimilation efficiency [equation (17)] at which biomass is transferred through several trophic levels. Thus, the assimilation efficiency and number of trophic levels represent the trophic structure of a community. Equation (18) or (19) provides a general relation between assimilation efficiency, trophic structure and the slope of a biomass spectrum. Here, several biomass spectra in different oceans and lakes at different seasons are chosen for elucidating applications of equations (18) and (19) to studies of community structures.

Sørfjorden, Norway

The same data set used in the section for growth and mortality estimates was applied to the analysis of trophic levels. The measurements were taken in the spring bloom during which enhanced primary production led to a fast growth of *C. finmarchicus*, a herbivorous copepod. The abundance of *C. finmarchicus* reached up to 1000 individuals m^{-3} (Edvardsen *et al.*, 2002). Their grazing on phytoplankton biomass represented the first trophic level. The dominant carnivorous organisms were chaetognaths (*Sagitta elegans*), which are up to 40 individuals m^{-3} (Zhou *et al.*, 2005). The best fitted linear slope is ~ –1.48 (Fig. 4), which leads to the number of recycles equal to 0.6 (60%), assuming the assimilation efficiency of 70%. Of the zooplankton mortality loss, 60% was recycled by carnivorous organisms, which implies that the zooplankton community was dominated by herbivorous zooplankton. Note that there is no justification for choosing the assimilation efficiency of 70% because there

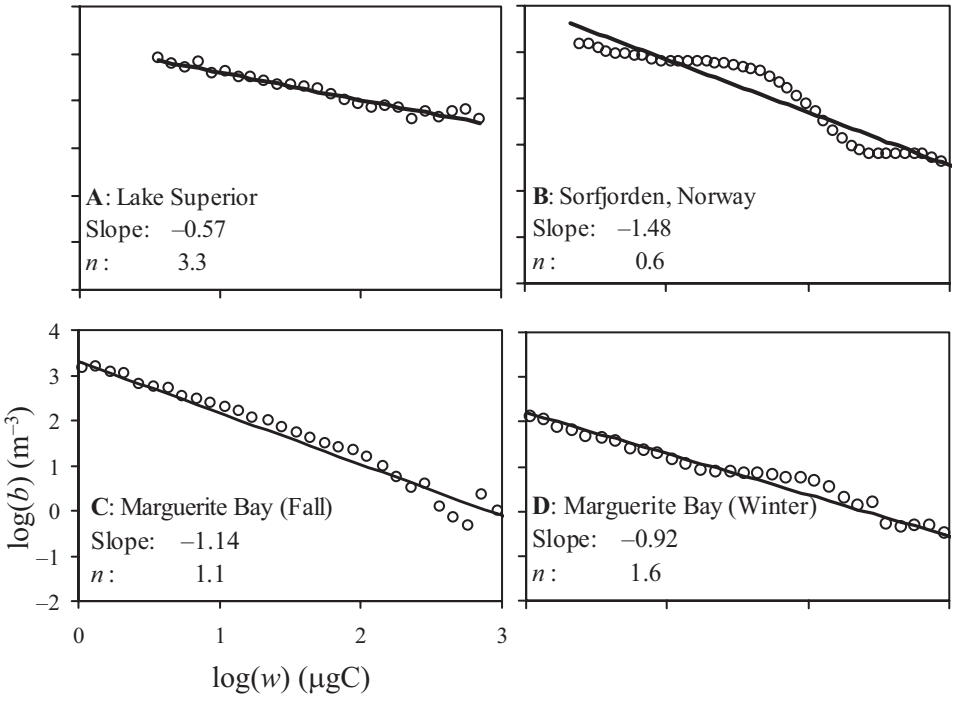

Fig. 4. Biomass spectra in m^{-3}, slopes and predicted numbers of internal biomass recycles (assuming the community assimilation efficiency of 0.7) versus body biomass in µgC within southeastern Lake Superior (**A**) off Michigan, Sørfjorden (**B**) in northern Norway and Marguerite Bay (**C** and **D**) west of Antarctic Peninsula. All axes are 10-based logarithmic.

Downloaded from https://academic.oup.com/plankt/article/28/5/437/1457472 by guest on 21 August 2022

is no community-assimilation efficiency estimate available for comparison. The estimate of the assimilation efficiency for marine copepods is the closet reference which is ~70% (Hirst and Lampitt, 1998).

Southeastern Lake Superior

A cruise was conducted using a towed integrated OPC and CTD system in the southeastern Lake Superior region east of Marquette, Michigan between 15 June and 20 June 1999 (Zhou *et al.*, 2001). Because of the seasonally northwesterly wind, a permanent warm water pool was formed near the coast which led to a permanent thermal stratification and subsurface chlorophyll maxima. Such a physical and biological setting is typically oligotrophic. The biomass spectrum slope is ~−0.57 (Fig. 4). If we assume that in this stable environment, zooplankton community had fully developed from herbivorous, small carnivorous to large carnivorous zooplankton, the biomass supplied into this system had to be recycled 3.3 times on the basis of equation (18), assuming the community-assimilation efficiency of 70%. Thus, the maintenance of such a flat biomass spectrum requires several trophic levels to recycle the biomass.

California Current

A SeaSoar (Chelsea Instruments) – OPC survey was conducted to understand the relationship between zooplankton distribution and physical fields in the California Current off the Oregon coast in June, 2001 (Fig. 5). The coastal upwelling area was found east of –128.4 W, which was separated by an upwelling front from the offshore stratified water. The high zooplankton abundance was found in the upwelling area which was distributed throughout the water column with a near surface maximum. The primary production was enhanced by upwelled nutrients which supported the dominant herbivorous zooplankton. The biomass spectrum of the coastal community is more complicated than a straight line. The dome centered at $10^{2.9}$ μgC represents a cohort in the size of euphausiid larvae propagating along the size spectrum. Removing this anomaly, the slope of the coastal community biomass spectrum had a mean of –1.8. Assuming the system assimilation efficiency of 70%, the internal energy would be recycled 0.4 time. In the offshore region, the water column was stably stratified with subsurface chlorophyll and zooplankton maxima beneath the thermocline. The slope of the offshore

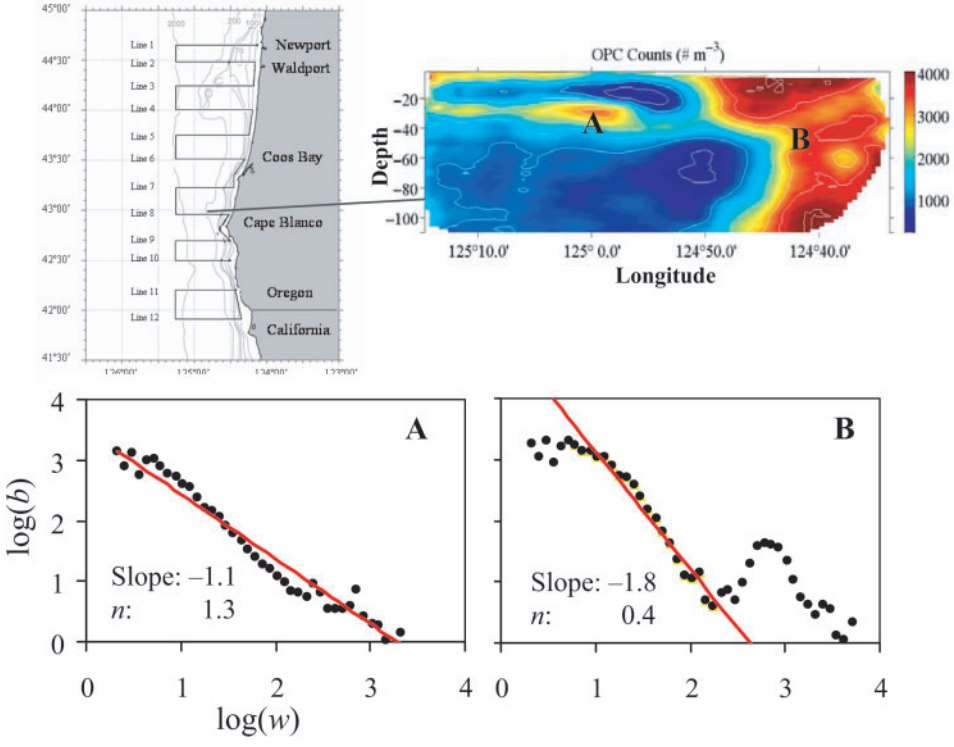

Fig. 5. Biomass spectra in m^{-3}, slopes and predicted numbers of internal biomass recycles (assuming the community assimilation efficiency of 0.7) in the offshore and near shore areas within California Current off Oregon marked by **A** and **B**, respectively. The black lines in the upper left panel indicate the cruise tracks, and the color image in the upper right panel represents the abundance in individuals m^{-3} along Transect 8 off Cape Blanco. All axes for biomass spectra are 10-based logarithmic.

Downloaded from https://academic.oup.com/plankt/article/28/5/437/1457472 by guest on 21 August 2022

community biomass spectrum was ~–1.1, and the biomass would be recycled 1.3 times, which implies carnivorous zooplankton were an important component in this well-developed stable community.

Marguerite Bay, west of Antarctic Peninsula

The biomass spectrum data were collected in Marguerite Bay and its vicinity by using an OPC mounted on the top of a Multiple Opening and Closing Nets and Environmental Sampling System (MOCNESS; B.E.S.S., Falmouth, MA, USA) during the 2002 Austral fall cruise on the A.S.R.V. *Laurence M. Gould* and the 2002 winter cruise on the R.V. *Nathaniel B. Palmer* (Zhou *et al.*, 2004). During a period of 90 days between these two cruises, the primary production was negligible, and the survival of mesozooplankton was dependent on feeding on other animals. During this period, 82% of biomass in the fall was consumed by the winter community. The system assimilation efficiency was estimated ~70% (Zhou *et al.*, 2004). The slopes of the fall and winter biomass spectra were found ~–1.14 and –0.92 (Fig. 4), and the internal biomasses were recycled 1.1 and 1.6 times, respectively. The increase in internal biomass recycles implies the increase in predation on internal biomass which transfers biomass from lower trophic to higher trophic levels.

Generalizing biomass spectrum theories

One of concerns in applying the biomass spectrum theories and OPC for obtaining biomass spectra for marine plankton is the overlapping in sizes between virus, bacteria, phytoplankton, zooplankton and nonliving particles. For example, diatom chains and marine snow overlap with small and mesozooplankton in sizes. In most cases, a specific model is developed for one specific functional group and methods have been developed to separate these different functional groups in laboratories, although it is practically difficult to define functional groups *in situ* or to take actually measurements at a high resolution. Automated instruments such as a Laser *In Situ* Scattering and Transmissometry Particle Size Analyzer (LISST, Sequoia Scientific Instruments, Bellevue, WA) for particles between 1 to 250 μm and a Laser Optical Plankton Counter (LOPC, Brooke Ocean Technologies, Dartmouth, Nova Scotia) for particles between 100 μm to 3 cm provide high-resolution measurements of all particles in water column, while they do not have the capability to separate functional groups. In some specific cases, it is possible to separate different functional groups in measurements made by an automated instrument relying on other independent methods. For example, preserving samples in sealed codends provided measurements of marine snow, which were used to correct the zooplankton measurements by an OPC (Heath *et al.*, 1999). Creating strong shear for breaking marine snow by towing an OPC at a high speed is another way to avoid marine snow contamination in zooplankton measurements (Edvardsen *et al.*, 2002). Recently, using the technology of still cameras, concentrations of marine snow can be efficiently removed from zooplankton biomass spectra (Herman, personal communication). But in general, a biomass spectrum provided by an OPC, LOPC or LISST represents the size structure of a mixture of different functional groups.

The biomass spectrum theories can be generalized for a mixture of all particles in water column. The biomass spectrum theories (Zhou and Huntley, 1997) rely on the two fundamental assumptions: (i) the sizes of particles will change due to growth or shrinkage and (ii) the number of particles will change due to any natural processes such as death, birth and division. The theories do no specify any processes for causing changes in body sizes and in numbers of particles. Thus, these theories can be directly applied to bacteria and phytoplankton which grow and then divide, contributing to changes in their numbers. Interpreting solutions of g and μ will depend on detailed analysis of dominant functional groups within a given size range. The composition of dominant functional groups may vary in different size ranges at different locations during different time.

Slope of a biomass spectrum: an inherent property of a community

To understand a plankton community and to predict its productivity require known process rates and community structure. To image a plankton community consisting of various plankton species and stages and their interlinked food web in a regional ocean, the plankton species compositions and food web links may vary in each m^3 so that any approach has to take averages to smooth details and variations forming functional groups. The questions to judge a valid approach are (i) will the averaging preserve biomass conservation and characteristics of the community structure and (ii) can those averaged variables be observed effectively *in situ*? The development of biomass spectrum observations and theories has been leading to (i) efficient *in situ* methods to measure biomass spectra and their spatiotemporal distributions (Herman, 1988; Huntley *et al.*, 1995; Tittel *et al.*, 1998; Quinones *et al.*, 2003; Herman *et al.*, 2004), (ii) *in situ* process rate estimates (Edvardsen *et al.*, 2002; Zhou and Huntley, 1997; Zhou *et al.*, 2004) and (iii) community trophic structure index developed in this manuscript.

How can the slope of a biomass spectrum represent the trophic structure? A number of size spectrum analyses on aquatic plankton communities indicate dome-like features for different functional groups (Dickie *et al.*, 1987; Sprules

Downloaded from https://academic.oup.com/plankt/article/28/5/437/1457472 by guest on 21 August 2022

et al., 1988, 1991; Kerr and Dickie, 2001). Each dome has a steep slope, and the combination of these different trophic domes leads to a less-steep linear community slope. The chain of trophic levels can be compared with a cluster of thermal engines which are interlinked through work and heat exchanges and are governed by the laws of thermodynamics. As the cluster of engines is set, its efficiency is determined by the number of interlinked engines and their efficiencies and is independent on external energy supplies. Hence, the amount of small plankton coming into the spectrum will determine the intercept, the height of a biomass spectrum. As the biomass propagates from small to large sizes, the biomass decreases following the biomass spectrum slope, while the slope is determined by the assimilation efficiency and number of trophic levels. Thus, the slope represents the inherent property of a plankton community.

ACKNOWLEDGEMENTS

This research was supported by the National Science Foundation grant numbers OCE0002257, OCE0238653 and OPP9910263 to M. Zhou. This is contribution No. 273 of the US GLOBEC Program.

REFERENCES

Andrews, K. J. H. (1966) The distribution and life-history of *Calanoides acutus* (Giesbrecht). *Disc. Rep.*, **34**, 117–162.

Atkinson, A., Meyer, B., Stubing, D. *et al.* (2002) Feeding and energy budgets of Antarctic krill *Euphausia superba* at the onset of winter-II. Juveniles and adults. *J. Limnol. Oceanogr.*, **47**, 953–966.

Atkinson, A. and Snyder, R. (1997) Krill–copepod interactions at South Georgia, Antarctica, I. Omnivory by Euphausia superba. *Mar. Ecol. Prog. Ser.*, **160**, 63–76.

Beyer, J. (1989) Recruitment stability and survival-simple size-specific theory with examples from the early life dynamics of marine fish. *Dana*, **7**, 45–147.

Brinton, E. and Townsend, A. (1991) Development rates and habitat shifts in the Antarctic neritic euphausiid *Euphausia crystallorophias*, 1986–87. *Deep-Sea Res.*, **38**, 1195–1211.

Carlotti, F. and Nival, S. (1992) Moulting and mortality rates of copepods related to age within stage: experimental results. *Mar. Ecol. Prog. Ser.*, **84**, 235–243.

Conover, R. J. (1988) Comparative life histories in the genera *Calanus and Neocalanus* in high latitudes of the northern hemisphere. *Hydrobiologia*, **167/168**, 127–142.

Dickie, L. M., Kerr, S. R. and Boudreau, P. R. (1987) Size-dependent processes underlying regulatiries in ecosytem structure. *Ecol. Monogr.*, **57**, 233–250.

Durbin, A. and Durbin, E. (1981) Standing stock and estimated production of phytoplankton and zooplankton in Narragansett Bay, Rhode Island. *Estuaries*, **4**, 24–41.

Edvardsen, A., Zhou, M., Tande, K. S. and Zhu, Y. (2002) Zooplankton population dynamics: measuring *in situ* growth and mortality rates using an Optical Plankton Counter. *Mar. Ecol. Prog. Ser.*, **227**, 205–219.

Fenchel, T. (1974) Intrinsic rate of natural increase: the relationship with body size. *Oecologia*, **14**, 317–326.

Heath, M. R. (1995) Size spectrum dynamics and the planktonic ecosystem of Loch Linnhe. *ICES J. Mar. Sci.*, **52**, 627–642.

Heath, M. R., Dunn, J., Fraser, J. G., Hay, S. J. and Madden, H. (1999) Field calibration of the Optical Plankton Counter with respect to *Calanus finmarchicus*. *Fish. Oceanogr.*, **8** (Suppl. 1), 13–24.

Herman, A. W. (1988) Simultaneous measurement of zooplankton and light attenuance with a new Optical Plankton Counter. *Cont. Shelf Res.*, **8**, 205–221.

Herman, A. W., Beanlands, B. and Phillips, E. F. (2004) The next generation of optical plankton counter: the Laser-OPC. *J. Plankton Res.*, **26**, 1135–1145.

Hirst, A. G. and Lampitt, R. S. (1998) Towards a global model of *in situ* weight-specific growth in marine planktonic copepods. *Mar. Biol.*, **132**, 247–257.

Hirst, A. G. and Sheader, M. (1997) Are *in situ* weight-specific growth rates body-size independent in marine planktonic copepods? *Mar. Ecol. Prog. Ser.*, **154**, 155–165.

Hopkins, T. L., Ainley, D. G., Torres, J. J. *et al.* (1993) Trophic structure in open waters of the marginal ice zone in the Scotia–Weddell confluence region during spring (1983). *Polar Biol.*, **13**, 389–397.

Huntley, M. and Boyd, C. (1984) Food-limited growth of marine zooplankton. *Am. Nat.*, **124**, 455–478.

Huntley, M. E. and Lopez, M. D. G. (1992) Temperature-dependent production of marine copepods: a global synthesis. *Am. Nat.*, **140**, 201–242.

Huntley, M. E., Nordhausen, W. and Lopez, M. D. G. (1994a) Elemental composition, metabolic activity and growth of Antarctic krill, *Euphausia superba* Dana, during winter. *Mar. Ecol. Prog. Ser.*, **107**, 23–40.

Huntley, M. E., Zhou, M. and Lopez, M. D. G. (1994b) *Calanoides acutus*. Gerlache Strait, Antarctica II. Solving an inverse problem in population dynamics. *Deep-Sea Res. II*, **41**, 209–227.

Huntley, M. E., Zhou, M. and Nordhausen, W. (1995) Mesoscale distribution of zooplankton in the California Current in late spring, observed by Optical Plankton Counter. *J. Mar. Res.*, **53**, 647–674.

Jorgensen, S. E. (1990) Ecosystem theory, ecological buffer capacity, uncertainty and complexity. *Ecol. Model.*, **52**, 125–133.

Jorgensen, S. E. (1994) *Fundamentals of Ecological Modeling*. Elsevier, Amsterdam-London-New York.

Kerr, S. R. and Dickie, L. M. (2001) *The Biomass Spectrum*. Columbia University Press, New York.

Longhurst, A. R. (1989) Pelagic ecology. Definition of pathways for material and energy flux. In Denis, M. M. (ed.), *Océanologie: Actualité et prospective*. Centre d'Océanologie de Marseille, Marseille, pp. 263–288.

Longhurst, A. R. (1991) Role of the marine biosphere in global carbon cycle. *J. Limnol. Oceanogr.*, **36**, 1507–1526.

Marchuk, G. I. (1975) *Methods of Numerical Mathematics*. Springer-Verlag, New York-Heidelberg-Berlin.

Miller, C. B., Frost, B. W., Batchelder, H. P. *et al.* (1984) Life histories of large, grazing copepods in a subarctic ocean gyre: *Neocalanus plumchrus*, *Neocalanus cristatus*, and *Eucalanis bungii* in the Northeast Pacific. *Prog. Oceanogr.*, **13**, 201–243.

Ohman, M. D. (1988) Predator-limited population growth of the copepod *Peseudocalanus* sp. *J. Plankton Res.*, **8**, 673–713.

Downloaded from https://academic.oup.com/plankt/article/28/5/437/1457472 by guest on 21 August 2022

Ohman, M. D. and Aksnes, D. L. (1996) The interrelationship of copepod fecundity and mortality. *J. Limnol. Oceanogr.*, **41**, 1470–1477.

Ohman, M. D. and Wood, S. N. (1996) Mortality estimation for planktonic copepods: *Pseudocalanus newmani* in a temperature fjord. *J. Limnol. Oceanogr.*, **41**, 126–135.

Platt, T. and Denman, K. (1978) The structure of pelagic marine ecosystems. *Rapp. P.-V. Réun. Cons. Int. Explor. Mer.*, **173**, 60–65.

Quinones, R. A., Platt, T. and Rodriguez, J. (2003) Patterns of biomass-size spectra from oligotrophic waters of the northwest Atlantic. *Prog. Oceanogr.*, **57**, 405–427.

Rodríguez, J. and Mullin, M. M. (1986) Relation between biomass and body weight of plankton in a steady state oceanic ecosystem. *J. Limnol. Oceanogr.*, **31**, 361–370.

Sheldon, R. W. and Parsons, T. R. (1967) A continuous size spectrum for particulate matter in the sea. *J. Fish. Res. Board Can.*, **24**, 909–915.

Sheldon, R. W., Prakash, A. and Sutcliffe, W. H. J. (1972) The size distribution of particles in the ocean. *J. Limnol. Oceanogr.*, **17**, 327–340.

Sheldon, R. W., Sutcliffe, W. H. and Paranjape, M. A. (1977) Structure of the pelagic food chain and the relationship between plankton and fish produciton. *J. Fish. Res. Board Can.*, **34**, 2344–2353.

Silvert, W. and Platt, T. (1978) Energy flux in the pelagic ecosystem: a time-dependent equation. *J. Limnol. Oceanogr.*, **23**, 813–816.

Sprules, W. G., Brandt, S. B., Stewart, D. J. *et al.* (1991) Biomass size spectrum of the Lake Michigan pelagic food web. *Can. J. Fish. Aquat. Sci.*, **48**, 105–115.

Sprules, W. G. and Munawar, M. (1986) Plankton size spectra in relation to ecosystem productivity, size, and perturbation. *Can. J. Fish. Aquat. Sci.*, **43**, 1789–1794.

Sprules, W. G., Munawar, M. and Jin, E. H. (1988) Plankton community structure and size spectra in the Gwogian Bay and North Channel ecosystems. *Hydrobiologia*, **163**, 135–140.

Sprules, W. G. and Stockwell, J. D. (1995) Size-based biomass and production models in the St Lawrence Great Lakes. *ICES J. Mar. Sci.*, **52**, 705–710.

Thiebaux, M. L. and Dickie, L. M. (1993) Structure of the body-size spectrum of the biomass in aquatic ecosystems: a consequence of allometry in predator–prey interactions. *Can. J. Fish. Aquat. Sci.*, **50**, 1308–1317.

Tittel, J., Zippel, B. and Geller, W. (1998) Relationships between plankton commmunity structure and plankton size distribution in lakes of northern Germany. *J. Limnol. Oceanogr.*, **43**, 1119–1132.

Zhou, M. (1998) Objective analysis of spatiotemporal distribution of zooplankton in the California current in later spring, 1993. *Mar. Ecol. Prog. Ser.*, **174**, 197–206.

Zhou, M. and Huntley, M. E. (1997) Population dynamics theory of plankton based on biomass spectra. *Mar. Ecol. Prog. Ser.*, **159**, 61–73.

Zhou, M., Zhu, Y. and Peterson, J. D. (2004) In situ growth and mortality of mesozooplankton during the austral fall and winter in Marguerite Bay and its vicinity. *Deep-Sea Res. II*, **51**, 2099–2118.

Zhou, M., Zhu, Y., Putnam, S. *et al.* (2001) Mesoscale variability of physical and biological fields in southeastern Lake Superior. *J. Limnol. Oceanogr.*, **46**, 679–688.

Zhou, M., Zhu, Y. and Tande, K. (2005) Circulation and behavior of euphausiids in Norwegian sub-Arctic fjords. *Mar. Ecol. Prog. Ser.*, **300**, 159–178.

Downloaded from https://academic.oup.com/plankt/article/28/5/437/1457472 by guest on 21 August 2022